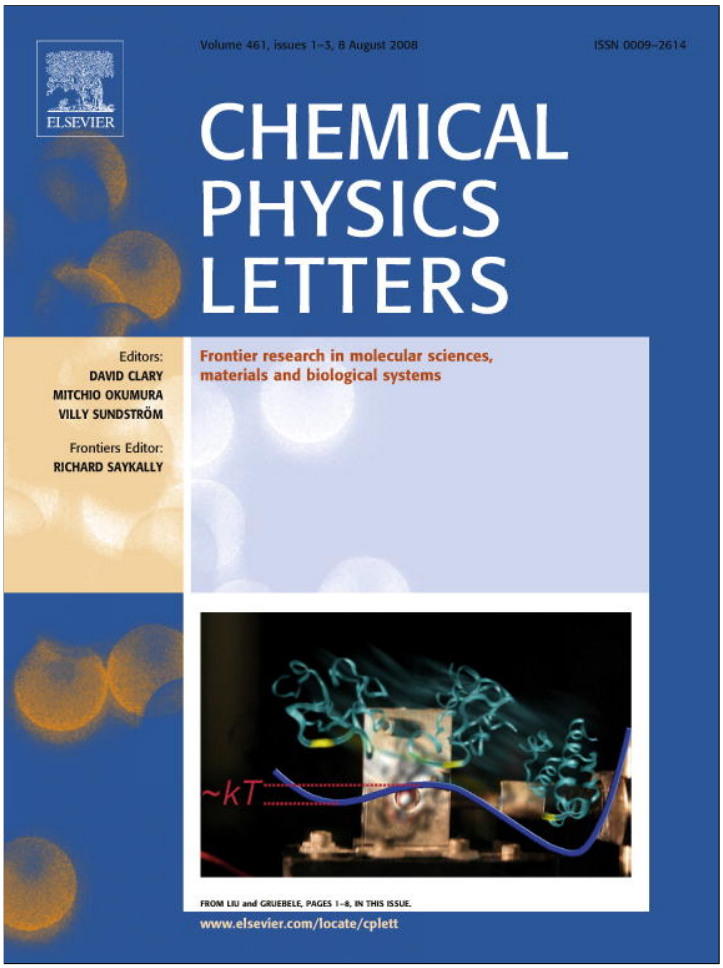

Chemical Physics Letters 461 (2008) 77–81

Contents lists available at ScienceDirect

Chemical Physics Letters

journal homepage: www.elsevier.com/locate/cplett

Time-resolved morphological study of organic thin film solar cells based on calcium/aluminium cathode material

B. Paci [a,*], A. Generosi [a], V. Rossi Albertini [a], P. Perfetti [a], R. de Bettignies [b], C. Sentein [c]

[a] Istituto di Struttura della Materia-Area di Ricerca di Tor Vergata, Via del Fosso del Cavaliere 100, 00133 Roma, Italy
[b] Commissariat à l'Energie Atomique, CEA Saclay, DRT-LITEN-DSEN-GENEC-L2C, F91191 Gif-sur-Yvette, France
[c] CEA Saclay, DRT-LITEN-DSEN-GENEC-L2C, F91191 Gif-sur-Yvette, France

ARTICLE INFO

Article history:
Received 29 April 2008
In final form 23 June 2008
Available online 1 July 2008

ABSTRACT

The stability and degradation of calcium/aluminium cathode organic solar cells are investigated *in situ* by time-resolved energy dispersive X-ray reflectometry. They combine the good charge carrier separation and transport properties of the poly(3-hexylthiophene-2,5-diyl):C_{61}-butyric acid methyl ester (P3HT:PCBM) bulk heterojunction blend and the capability of the calcium/aluminium cathode to improve the fill factor and the open circuit voltage, with respect to aluminium cathodes cells. The study focuses on the crucial problem of the device structural/morphological stability in working condition. It aims to detect and control possible morphological variations at the various interfaces and to correlate these changes to the device aging.

1. Introduction

The latest advances in the field of plastic solar cells have brought these very promising devices to a level at which commercialisation is a realistic prospect. At present, organic PV devices reach power conversion efficiencies as high as 6.1% [1–5] and studies of their stability are now beginning to focus on the materials aging [6,7], the choice of the electrode [8] and the effect of encapsulation [9]. This research led to an increase of the lifetimes, up to 2000 h in the continuous operation mode [10].

The active layer of the cells investigated in the present study consisted of donor–acceptor bulk heterojunctions obtained by blending two organic materials, one acting as electron donor and the other as electron acceptor. The high efficiency recently reached by these devices is due to a molecular approach to PV conversion, based on photoinduced ultra-fast electron transfer from a conjugated polymer to fullerene [11,12]. In the present case, poly(3-hexyl thiophene), widely studied for its semiconducting properties and, currently, for its applications in photovoltaics, is used as the donor material [13,14]. Moreover, the use of calcium/aluminium cathode allows to improve the cell fill factor and the open circuit voltage, with respect to cells using a simple aluminium cathode. However, further improvements are required with regard to device lifetime [15,16].

A key strategy to achieve this goal focuses on the optimization of the cell architecture and, in particular, on the study of the coupling of the active layer with various electron transport materials, as well as on the choice of the most suitable cathode. Indeed, the cell stability under both storage and working conditions is strongly affected by phenomena that may well occur at the interfaces between various layers. As a consequence, it is of the highest importance to detect possible reaction or diffusion processes that involve the different elements constituting these 'sandwich-like' systems, and that can be detrimental for their lifetime [17–19].

In this framework, the present study aims to validate the use of the proposed X-ray technique for detecting interface morphological degradation phenomena, possibly occurring in working polymer PV devices.

2. Experimental methods

The cells studied are provided with an indium tin oxide (ITO) substrate, cleaned in an ultrasonic bath with acetone, isopropanol and rinsed in de-ionized water, dried in an oven and finally treated with UV-ozone. The ITO layer was spin-coated with a 50 nm film of poly(3,4-ethylenedioxythiophene)–poly(styrenesulfonate) PEDOT:PSS (Baytron PH®). The active layer of P3HT:PCBM was deposited by spin-casting from an anhydrous chlorobenzene solution. The top contact consisted of a metallic Ca layer, sealed by means of an aluminium cap layer both deposited at a pressure of 7×10^{-7} mbar. This value was chosen to obtain the best contact between the Ca film and the organic layer, heavily dependent on the pressure in the chamber [20]. All the cells have an active surface of 32 mm^2.

The experiments were based on the energy dispersive X-ray reflectometry (EDXR) technique, which is very effective for *in situ* non-destructive investigations of surface and interface properties

* Corresponding author. Fax: +39 06 4993 4153.
E-mail address: barbara.paci@ism.cnr.it (B. Paci).

0009-2614/$ - see front matter © 2008 Elsevier B.V. All rights reserved.
doi:10.1016/j.cplett.2008.06.070

of thin films and layered samples [13–16]. The theory of the ED method, together with an overview of its applications is described in Refs. [21,22]. Essentially, in the small angle approximation and far from the absorption edges of the constituting materials, an X-ray reflectivity pattern represents the reflected intensity as a function of the scattering parameter q. The latter is defined as $q = 4\pi\sin\theta\lambda = (2/hc)E\sin\vartheta$, were ϑ is the deflection angle, λ is the X-ray incident wavelength, E is the radiation energy, h is Plank's constant and c is the velocity of light.

Since the scattering parameter q depends on both the reflection angle and the energy of the X-rays, it enables the reflectivity measurement to be performed using a polychromatic beam and an energy scan by means of an energy sensitive detector (energy dispersive mode) may be carried out as an alternative method to the conventional angular dispersive mode, (which makes use of a fixed X-ray energy and explores the reciprocal space by an angular scan).

The morphological parameter (namely the film thickness d and its roughness σ) can be obtained by a fit of the data reflectivity pattern.

The experimental apparatus consisted of a non-commercial reflectometer [21,22] supplied with a tungsten anode X-ray tube and of an energy sensitive detector (a EG&G high purity germanium solid-state detector, with 1.5–2% energy resolution in the 15–50 keV energy range used). These two components are mounted on two opposite benches pivoting around a common central axis. The optical path of the X-ray beam is defined by four adjustable slits. The Bremmsstrahlung of the X-ray tube (3 kW power, tungsten anode) is used as the polychromatic X-ray probe and the measurements are performed in static conditions, neither monochromator nor goniometer being needed.

3. Results and discussion

The energy dispersive X-ray reflectometry technique was applied *in situ* to investigate the device's morphological changes in working conditions. Evidence of a degradation effect was found. In order to interpreter the origin of this phenomenon a systematic study was performed on a series of calcium electrode based devices of selectively modified structure.

In particular, the calcium electrode of the cells investigated in the present study is in direct contact with the organic film and is sealed by an aluminium cap layer. The aluminium layer is essential to prevent calcium oxidation, produced by the contact with ambient water vapour and oxygen. Moreover, since the organic materials used as active layers may also degrade under atmospheric conditions, encapsulation with a barrier material (characterized by low permeation rates for water vapour and oxygen) is very useful. It follows that a crucial point to be addressed, in the attempt to enhance the durability of the devices performances over time, is the joint effect of the morphological stability at both the calcium-active layer interface and the aluminium–calcium interface (see Fig. 1).

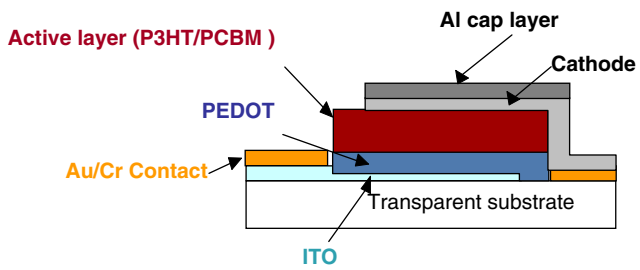

Fig. 1. Sketch of the cell structure.

The samples, deposited under controlled atmosphere, were initially exposed to air (by storage in the dark at ambient conditions) for one day. Then, they were measured under controlled atmospheric conditions (N_2 gas flux) during illumination. The investigation was carried out in several steps.

3.1. Monitoring the stability of the aluminium cap layer in working conditions

A first *in situ* experiment aimed to detect any possible photoinduced modification of the Al/Ca interface morphology. It was carried out on a device (cell #1) with the following structure: glass/ITO/PEDOT:PPS/P3HT:PCBM/Ca/Al. A large number of X-ray reflection patterns were collected (Fig. 2). In the first part of the experiment, the cell was kept in the dark (bottom pattern) and, then it was illuminated by a white light lamp (10 mW/cm^2) for several hours. An experimental procedure was used to maximize the Al signal with respect to that coming from the other layers, which consisted of tilting the sample slightly under the X-ray beam, by means of a rocking cradle. In this way, it was possible to assign the Kiessig fringes visible in Fig. 2, to the Al film alone. The thickness d of the film is obtained, together with its roughness σ, by a Parratt fit [23], suitably modified the energy dispersive mode [21]:

$$|R|^2 = \{1 - 2[(\mathrm{Real}(R_l * R_r - R_l R_r)\exp(-2kd)] / [1 + \exp(-4kd) - 2\mathrm{Real}(R_l R_r)\exp(-2kd)]\}$$

where $R_l = (k_0 - k)/(k_0 + k)$ is the Fresnel film reflectivity, $R_r = (k - k_s)/(k + k_s)$ is the Fresnel substrate reflectivity, $k_0 = q/2$ is the radiation wave number in air and d is the film average thickness.

The quantities k and k_s are the radiation wavenumbers in the film and in the substrate, respectively, which depend on k_0

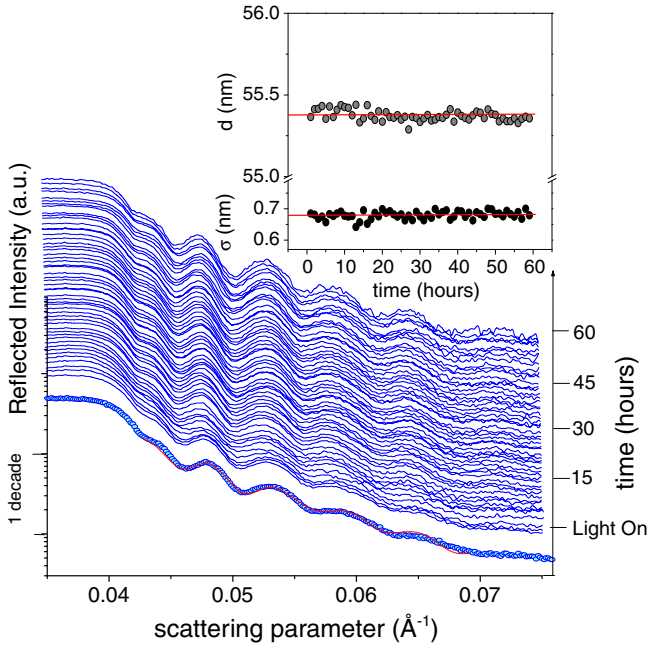

Fig. 2. Reflectivity profiles, shifted in height for clarity, relative to the Ca/Al interface for cell #1 (glass/ITO/PEDOT:PSS/P3HT:PCBM/Ca/Al structure) collected under controlled atmosphere in the dark (bottom pattern) and upon illumination. All the patterns were fitted using the Parratt's model (the comparison of the fit with the data is reported for the bottom spectrum, as an example) providing the values of the morphological parameters. The curves of the Al film thickness and roughness as a function of time, obtained by fitting all the EDXR patterns, are reported in the inset.

$k_f = (k_0^2 - 4\pi\rho)^{1/2}$ and $k_s = (k_0^2 - 4\pi\rho_s)^{1/2}$

When the surface or the interfaces are not sharp, the reflected intensity decrease due to roughness is taken into account by introducing a Debye Waller like factor (Nevot-Croce factor [24]). Recent results have shown the suitability of this model to interpret time-resolved EDXR measurements of P3HT:PCBM bulk heterojunctions in organic solar cells upon illumination [25].

As it can be noticed, the patterns of this sequence overlap. Since no change in the oscillation period occurs, the morphology of the Al cap layer does not undergo any modification upon working conditions of the device. In particular, both the surface of the aluminum layer and its interface with the calcium one are stable during illumination. This is confirmed by the results of the data fits, i.e. the Al film thickness and roughness vs time curves are both constant (see the inset). It is worth mentioning that the high resolution of the EDXR patterns allowed for an elevated accuracy in the data analysis, as shown by the comparison of the fit with the data for the bottom spectrum in Fig. 2. In particular, for the film thickness, the relative error in the Parratt fit is the order of 0.2%.

3.2. Monitoring the stability of the calcium electrode in working conditions

A second critical point addressed concerned the aging of the interface between the active layer and the Ca electrode. To retrieve information on the cathode morphological stability, a new device, having the same structure of the previous one, was fabricated and measured *in situ* (cell #2). The results are shown in Fig. 3. The same experimental procedure adopted previously was now applied to maximize the Ca layer contribution. It can be noticed that the patterns reported in Fig. 3 show a characteristic deformation of the Kiessig fringes intensity, particularly visible in the case of the fourth oscillation. This effect can be easily explained in terms of beats between the X-ray reflection produced by the two films, i.e. the cathode and the aluminium layer. The reflection pattern of each film, as discussed above, consists of an oscillating signal whose frequency is proportional to the inverse of the film thickness. Since the films have similar thicknesses, the two oscillations interfere producing an amplitude modulation (see the inset in Fig. 3).

While the cell is being illuminated, a change in the EDXR profiles occurs. The modification of the patterns is hardly visible by the naked eye. The main effect is a change in the frequency of the Kiessig fringes, evidenced in the inset of Fig. 3, showing the purely oscillating contribution of the first (black) and last (red) pattern. Once data analysis is performed a quantitative information on the morphological changes over time is obtained. The evolution of the Ca cathode thickness d and its roughness σ over time, obtained by processing of the EDXR patterns is reported in Fig. 4a. The d vs t curve is well described by a simple Boltzman sigmoidal fit, $d(t) = d_1 + (d_2 - d_1)\,(1 - \exp-(t/\tau))$, which indicates that the film thickness increases from its original value $d_1 = 493.3 \pm 0.5$ Å to an asymptotical value $d_2 = 501.4 \pm 0.5$ Å, in a characteristic time τ_1 of 20 h.

Therefore, the result of this second experiment is that a modification in the EDXR profiles occurs, witnessing an increase of the Ca thickness as a consequence of the exposure to light. It follows that the latter effect needs to be interpreted and, possibly, inhibited.

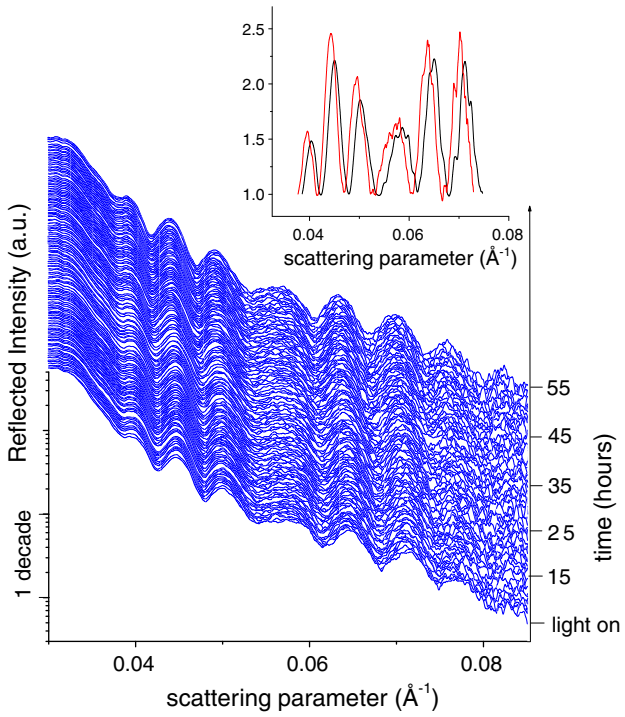

Fig. 3. Reflectivity profiles, shifted in height for clarity, relative to the Ca/active layer interface for cell #2 (glass/ITO/PEDOT:PSS/P3HT:PCBM/Ca/Al structure) collected under controlled atmosphere and upon illumination. The inset shows the purely oscillating contribution of the first (black) and last (red) pattern. (For interpretation of the references to colour in this figure legend, the reader is referred to the web version of this article.)

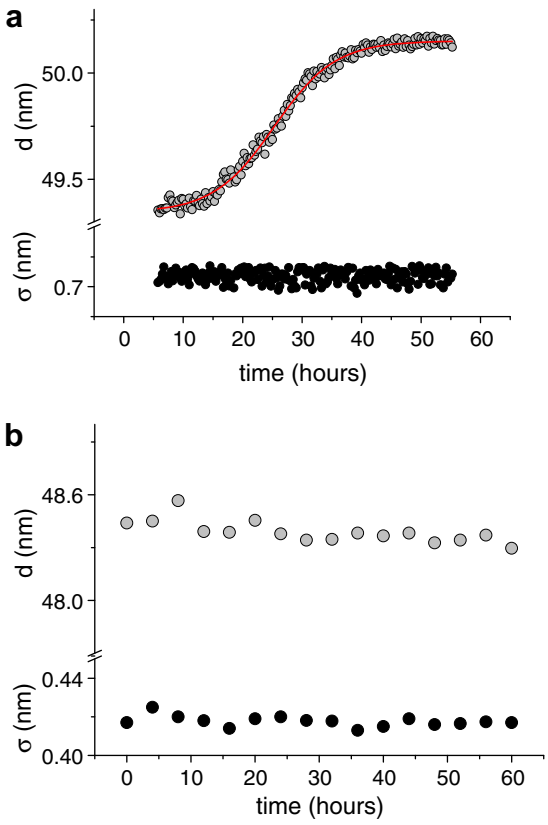

Fig. 4. (a) Curves of the Ca electrode thickness and roughness, obtained by fitting all the EDXR patterns of Fig. 3, as a function of time (cell #2, glass/ITO/PEDOT:PSS/P3HT:PCBM/Ca/Al structure). The solid line represent the fit of the data points by a Boltzman curve. (b) Results of the EDXR measurements for cell #3 (glass/ITO/P3HT:PCBM/Ca/Al structure): curves of the Ca film thickness and roughness as a function of time.

3.3. Enhancing the devices morphological stability in working conditions

The main questions arising from these experimental results concern the possibility of individuating the cause of the observed morphological changes of the calcium layer and of verifying to what extent they are connected to aging effects.

Some general considerations can be made in this respect:

A first possible explanation may be that the heating during illumination promotes the diffusion of calcium ions in the polymer so that an interface layer, consisting of a solution of calcium in the organic film, may be formed. In fact, a similar phenomenon has already been detected during the deposition of OLED based on PPV [26]. In our case, since the EDXR technique is sensitive to the contrast between the scattering length densities of adjacent layers stacked in the device, the observed increase in the metal electrode thickness would correspond to the formation of a thin layer at the Ca-organic film interface characterized by an electronic scattering length density very close to that of pure calcium [27]. Strictly speaking, an increase in density of the organic film at the interface with the Ca layer, due to diffusion of Ca ions, should be accompanied by a lowering in the electrode density. The latter, in principle, would be revealed as a change in the position of the total reflection edge in the EDXR patterns. However, in the present case, since the Ca thickening is of the order of 2% only, it would produce effects well below the detection threshold of the EDXR technique and no relevant change in the patterns profile is expected.

An alternative explanation could be the occurrence of another phenomenon, induced by illumination, namely calcium oxidation. Indeed, calcium is known to rapidly undergo an oxidation process when exposed to oxygen and moisture, which leads to the formation of a thin insulating oxide barrier [28]. In our case, since no passivating layer is expected to be initially present, because the deposition is performed in a controlled atmosphere, an oxidation process of the calcium layer may develop during the cell working. Nevertheless, the oxidation of the calcium film may occur only in the case that both oxygen and water being available to concur to the oxidation process, since calcium does not react with oxygen in dry atmosphere conditions [29,30]. This is the case of the PV cells under study. Indeed, the calcium layer in the device is in contact with the oxygen ions (bounded to the polymers of the organic layer), which may be released during illumination, and photo-induced oxidation may well occur. On the other hand, the organic film was deposited on a PEDOT:PSS film, which may retain some water from the deposition process.

The increase of the cathode thickness revealed by the EDXR study may therefore be attributed to the formation of a CaOx layer, characterized by an optical density close to that of the Ca film.

In the following section we discuss how the use of *in situ* EDXR enables the discrimination between the two hypotheses.

In order to verify whether the degradation of the calcium layer is caused by the oxidation of the Ca buried interface or to the calcium ions diffusion process, a new cell, with the following structure glass/ITO/P3HT:PCBM/Ca/Al (cell #3) was measured by EDXR. In this case, since no PEDOT:PSS layer is used, no residual water is expected to be present in the device. The results are shown in Fig. 4b, in which the curves of the Ca film thickness and roughness as a function of time are reported. It can be noticed that the Ca layer does not undergo any modification upon working conditions.

The result of the experiment on cell #3 indicate that the observed morphological instability of cell #2 was therefore due to the oxidation of the metallic Ca electrode, promoted by the presence of moisture and allows the hypothesis of diffusion of calcium ions into the organic layer to be rejected. At this point, our investigation focused on the quantification of the effect on the device performances of the Ca electrode morphology.

3.4. Effect of the morphology on the device's efficiency and aging

In order to quantify the damage produced by the Ca electrode degradation process, two new cells were assembled and electrically characterized under controlled atmospheric conditions. The layer stacks were equivalent to those of the previous cells, used for the EDXR characterization (glass/ITO/PEDOT:PPS/P3HT:PCBM/Ca/Al):

- (Cell #4) glass/ITO/PEDOT:PPS/P3HT:PCBM/Ca/Al, i.e. equivalent to cell #1 and cell #2.
- (Cell #5) glass/ITO/P3HT:PCBM/Ca/Al, i.e. equivalent to cell #3,(no PEDOT:PPS layer).

Comparison of the efficiency vs time curves for the above devices, under simulated AM1.5 80 mW/cm^2 illumination, are reported in Fig. 5. The starting efficiency of the cell using the PEDOT:PPS layer (cell #4) was an order of magnitude higher with respect to that of the cell without the PEDOT:PPS layer (cell #5). This is probably due to the fact that the PEDOT:PPS layer is able to improve the contact between the ITO electrode and the organic film, first by smoothing the ITO surface and, secondly, by better adapting the energy levels or lowering the energy barrier [31]. On the other hand, cell #4 underwent a rapid fading and after 60 h of working its efficiency dropped to less than 20% of its initial value and was comparable to that of cell #5. The curve relative to cell #4 is well fitted by a fast exponential decay with a characteristic time of 20 h, namely the same characteristic time of the photoinduced electrode degradation process observed by EDXR.

Therefore, this study reports evidences that that the oxidation of the metallic Ca electrode, observed by EDXR, caused a rapid decrease in the efficiency of the device having a PEDOT:PPS underlayer.

In order to combine the good morphological stability device, observed in the absence of residual moisture, with an enhanced starting efficiency, post deposition thermal treatments where applied on devices using a PEDOT:PPS underlayer. As an example, the aging curve corresponding to a cell annealed at 110 °C for 5 min is re-

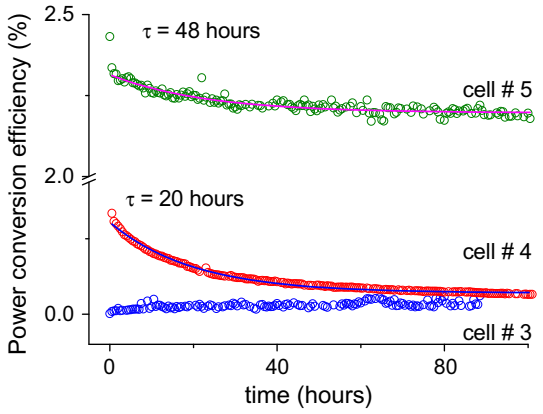

Fig. 5. Efficiency vs time curves for the following cells: Cell #4: glass/ITO/PEDOT:PPS/P3HT:PCBM/Ca/Al (in green). Cell #5: glass/ITO/P3HT:PCBM/Ca/Al (in blue). Cell #6: glass/ITO/PEDOT:PPS/P3HT:PCBM/Ca/Al, after post deposition annealing at 110 °C for 5 min (in red). (For interpretation of the references to colour in this figure legend, the reader is referred to the web version of this article.)

ported in Fig. 5. The starting efficiency of this device (cell #6), was seven times higher with respect to that of the pristine cell of the same structure (cell #5). This is due to concomitant factors, among them the fact that the annealing procedure probably leads to a better organisation of the material, which improves the charge mobility and, therefore, the cell efficiency.

Moreover, the annealed cell (cell #6), was essentially stable over time and after 60 h its efficiency was reduced by 6% only, indicating that no moisture was present in the PEDOT:PPS layer.

4. Conclusions

In conclusion, the degradation and stability in working conditions of polymer PV devices with calcium electrodes was investigated. The approach used was based on the real time monitoring of the morphological changes occurring at the various interfaces of the 'sandwich like' structure of the cells, both in the dark and during illumination, and allowed the detection of undesirable aging effects. In particular, the Al cap layer was found to be unaffected by exposure to light, its morphology being stable over time. Conversely, the Ca electrode was shown to be unstable, an increase of the Ca layer thickness occurring in working conditions. This effect was attributed to the degradation of the calcium electrode from a metallic to an oxidized state. Furthermore, the study of a cell with a suitably modified structure demonstrated that this oxidation process is related to the presence of water molecules inside the cell, residual from the PEDOT:PSS underlayer deposition. The effect of residual moisture was inhibited by depositing the organic film directly onto the ITO electrode.

The observed morphological instability of the electrode buried interface was correlated to cell aging. It was shown that post deposition thermal treatments result in a significant improvement of both the initial efficiency and the stability of the device.

References

[1] G. Li, V. Shrotriya, J.S. Huang, Y. Yao, T. Moriarty, K. Emery, Y. Yang, Nature Mater. 4 (2005) 864.
[2] Y. Kim et al., Nature Mater. 5 (2006) 197.
[3] J. Peet, J.Y. Kim, N.E. Coates, W.L. Ma, D. Moses, A.J. Heeger, G.C. Bazan, Nature Mater. 15 (2007) 1617.
[4] K. Kim, J. Liu, M.A.G. Namboothiry, D.L. Caroll, Appl. Phys. Lett. 90 (2007) 163511.
[5] W. Ma, C. Yang, X. Gong, K. Lee, A.J. Heeger, Adv. Funct. Mater. 15 (2005) 1617.
[6] F.C. Krebs, H. Spanggaard, Chem. Mater. 17 (2005) 5235.
[7] S. Chambon, A. Rivaton, J.L. Gardette, M. Firon, L. Lutsen, J. Polym. Sci., A – Polym. Chem. 45 (2007) 317.
[8] R. de Bettignies, J. Leroy, M. Firon, C. Sentein, Synth. Met. 156 (2006) 510.
[9] C.J. Brabec, J.A. Hauch, P. Schilinsky, C. Waldauf, MRS Bull. 30 (2005) 502.
[10] F.C. Krebs, Sol. Energy Mater. Sol. Cells 90 (2006) 36333.
[11] N.S. Sariciftci, L. Smilowitz, A.J. Heeger, F. Wudl, Science 258 (1992) 1474.
[12] C.J. Brabec, G. Zerza, G. Cerullo, S. De Silvestri, S. Luzzati, J.C. Hummelen, N.S. Sariciftci, Chem. Phys. Lett. 340 (2001) 232.
[13] A.J. Mozer et al., J. Phys. Chem. B 108 (2004) 5235.
[14] S.E. Shaheen, C.J. Brabec, N.S. Sariciftci, F. Padinger, T. Fromherz, J.C. Hummelen, Appl. Phys. Lett. 78 (2001) 841.
[15] S. Schuller, P. Schilinsky, J. Hauch, C.J. Brabec, Appl. Phys. A 79 (2004) 37.
[16] P. Schilinsky, C. Waldauf, J. Hauch, C.J. Brabec, Thin Solid Films 451 (2004) 105.
[17] X.N. Yang et al.Nano Lett. 5 (2005) 579.
[18] B. Paci et al., Appl. Phys. Lett. 87 (2005) 194110.
[19] B. Paci et al., Appl. Phys. Lett. 89 (2006) 043507.
[20] P. Bröms, J. Birgersson, N. Johansson, M. Lögdlund, W.R. Salaneck, Synth. Met. 74 (1995) 179.
[21] V. Rossi Albertini, B. Paci, A. Generosi, J. Phys. D – Appl. Phys. 39 (2006) 461.
[22] R. Caminiti, V. Rossi Albertini, Int. Rev. Phys. Chem. 18 (1999) 263.
[23] L.G. Parrat, Phys. Rev. 95 (1954) 359.
[24] L. Névot, P. Croce, R. Phys. Appl. 15 (1980) 761.
[25] B. Paci, A. Generosi, V. Rossi Albertini, R. Generosi, P. Perfetti, R. de Bettignies, C. Sentein,, J. Phys. Chem. doi:10.1021/jp801674v.
[26] G.G. Andersson et al., J. Phys. D: Appl. Phys. 35 (2002) 1103.
[27] S.J. Roser, R. Felici, A. Eaglesham, Langmuir 10 (1994) 3853.
[28] L.M. Do et al., J. Appl. Phys. 76 (1994) 5118.
[29] P.E. Burrows et al., Displays 22 (2001) 65.
[30] P. Pascal, in: Nouveau traité de chimie minérale, vol. 4, Paris, Masson, p. 412.
[31] Y. Cao, Synth. Met. 87 (1987) 171.